Coarsening on percolation clusters: out-of-equilibrium dynamics versus nonlinear response

1998 J. Phys. A: Math. Gen. 31 5203

(http://iopscience.iop.org/0305-4470/31/23/004)

J. Phys. A: Math. Gen. **31** (1998) 5203–5217. Printed in the UK PII: S0305-4470(98)91445-7

Coarsening on percolation clusters: out-of-equilibrium dynamics versus nonlinear response

P Butaud† and R Mélin‡

Centre de Recherches sur les Très basses températures§ (CRTBT-CNRS), Laboratoire conventionné avec l'Université Joseph Fourier BP 166X, 38042 Grenoble Cédex, France

Received 6 February 1998

Abstract. We analyse the violations of linear fluctuation–dissipation theorem (FDT) in the coarsening dynamics of the antiferromagnetic Ising model on percolation clusters in two dimensions. The equilibrium magnetic response is shown to be nonlinear for magnetic fields of the order of the inverse square root of the number of sites. Two extreme regimes can be identified in the thermoremanent magnetization: (i) linear response and out-of-equilibrium relaxation for small waiting times (ii) nonlinear response and equilibrium relaxation for large waiting times. The function $X(C)$ characterizing the deviations from linear FDT crossovers from unity at short times to a finite positive value for longer times, with the same qualitative behaviour whatever the waiting time. We show that the coarsening dynamics on percolation clusters exhibits stronger long-term memory than usual Euclidean coarsening.

1. Introduction

Ageing experiments in spin glasses [1, 2] first carried out by Lundgren *et al*, have generated a large amount of experimental as well as theoretical work. For a review on recent theoretical developments in this field, we refer the reader to [3]. Two types of experiments have been investigated: the zero-field-cooled experiment and the thermoremanent magnetization experiment, both leading to similar results. In this paper, we shall restrict ourselves to the thermoremanent magnetization experiment, consisting of first quenching the system below its glass transition temperature at time $t = 0$, applying a small constant magnetic field up to the waiting time t_w, switching off the magnetic field at time t_w, and measuring the magnetization relaxation at time $t_w + \tau$. It is an experimental observation that the magnetization relaxation depends on the 'age' of the system, namely, on the waiting time. Different theoretical approaches have been developed to date, for instance: droplet picture [4, 5], mean-field models [6] or phenomenological trap models [7]. Several scenarios have been proposed, such as 'true' versus 'weak' ergodicity breaking [7], or 'interrupted' ageing [7]. The first two scenarios depend on whether ergodicity breaking occurs for finite or infinite waiting times. 'Interrupted' ageing means that, at a finite temperature, there is no longer ageing if the waiting time is larger than finite (but possibly large) timescale. In other words, the system equilibrates in a finite time.

Ageing can be characterized by the violation of the fluctuation–dissipation theorem (FDT). If the system has reached thermodynamic equilibrium before the magnetic field

† E-mail address: butaud@crtbt.polycnrs-gre.fr
‡ E-mail address: melin@crtbt11.polycnrs-gre.fr
§ UPR 5001 du CNRS.

0305-4470/98/235203+15$19.50

is switched off at time t_w, the magnetization response is then independent on t_w. This situation can be realized either at large temperatures, or in an 'interrupted ageing' situation (which will be the case in this paper), or, in the presence of non-interrupted ageing, by formally taking the limit $t_w \to +\infty$ before the thermodynamic limit $N \to +\infty$. Then, the equilibrium thermoremanent magnetization $m(\tau)$ is related in a simple fashion to the autocorrelation of the spin configurations at times t_w and $t_w + \tau$ via the FDT (see section 3 for more details). In out-of-equilibrium dynamics, the FDT is no longer valid, and there are analytical predictions in some mean-field solvable models of what the FDT violation is [6, 8, 9]. In particular, Cugliandolo and Kurchan [6] proposed that the out-of-equilibrium linear response kernel $R(t, t')$ relating the magnetization to the correlation depends on t and t' only through the autocorrelation $C(t, t')$. The FDT violation is then characterized by a function $X(C)$ that depends only on the autocorrelation, and, as recalled in section 3, can be obtained from the thermoremanent magnetization simulations.

The aim of this paper is to study the FDT violation in dilute Ising antiferromagnets at the percolation threshold, with a Hamiltonian

$$H = J \sum_{\langle i,j \rangle} \sigma_i \sigma_j \tag{1}$$

where the summation is carried out over neighbouring pairs of spins on a percolation cluster. In practice, we shall only study here percolation clusters generated on a square lattice in a two-dimensional space. It is well known that, for a finite cluster of N sites, the dynamics freezes as the temperature decreases below the glass crossover temperature [10]

$$T_g = \frac{2J\bar{d}\nu_P}{\ln N} \tag{2}$$

with $\bar{d}$ the fractal dimension and ν_P the percolation exponent. This glass crossover originates from the conjugate effect of large-scale 'droplet' excitations (with zero-temperature energy barriers that scale like $J \ln N$ [11, 12]), and the divergence of the correlation length at low temperatures [13].

It is of interest to understand the FDT violation in these systems for two reasons. First, a quite different behaviour from Euclidean coarsening is expected, with more pronounced long-term memory effects owing to the slow dynamics of 'droplet' excitations. We shall indeed show that the function $X(C)$ characterizing the fluctuation–dissipation ratio crossovers from unity to a smaller value X_0 in the ageing regime. Whereas X_0 is zero in Euclidean coarsening, we find a non-zero value for coarsening on percolation clusters. This indicates that, even though these non-frustrated systems show interrupted ageing, the FDT violation in these systems shares some common features with the behaviour of spin-glass models in three [18] and four [19] dimensions. The second motivation for studying these systems is, as shall be developed in section 2, that the low-temperature magnetic response to an external magnetic field is linear only for magnetic fields smaller than a typical field h^* scaling like $T/\sqrt{N}$ (see section 2). One is thus led to study the FDT violation in the absence of linear response to an external magnetic field.

This paper is organized as follows. Section 2 is devoted to analysing the equilibrium magnetic response to an external magnetic field and to show that the low-temperature equilibrium response is nonlinear. Section 3 recalls how the function $X(C)$ characterizing the FDT violation can be obtained from the thermoremanent magnetization experiment. The results of our simulations are presented and discussed in section 4. Section 5 is devoted to some final remarks.

2. Absence of linear response at low temperature

In this section, we analyse the low-temperature equilibrium response to an external magnetic field. We consider a percolating cluster of N sites, and first analyse a toy-model for the magnetization response to an external magnetic field. The equilibrium magnetization $M(h)$ in an external magnetic field h can be expressed as

$$\overline{M(h)} = \frac{\overline{\partial \ln\langle \exp(\beta h M)\rangle_0}}{\partial(\beta h)} \tag{3}$$

where $\langle X\rangle_0$ denotes the thermal average of the observable X with respect to the system without a magnetic field, and $\overline{X}$ denotes the disorder average.

We are first going to formulate in section 2.1 a low-temperature toy-model which allows analytical calculations of (3). The predictions from this toy-model will be compared with simulations in section 2.3.

2.1. Formulation of the low-temperature toy-model

Our toy-model relies on some assumptions about the geometry of the percolating clusters, and further assumptions about the low-temperature magnetization distributions. The validity of these assumptions relies on the fact that some of the predictions of our toy-model can be successfully compared with simulations (see section 2.3).

In the dilute antiferromagnet model (1), the magnetization of the Néel state of the percolating cluster is equal, up to a sign, to the difference $\Delta = N_A - N_B$ in the number of sites in the two sublattices A and B, the number of sites in the percolating cluster being $N = N_A + N_B$. In order to allow for analytic treatment, we assume that both N_A and N_B are independent variables and Gaussian distributed according to

$$P(N_{A,B}) = \frac{1}{\sqrt{2\pi}\sigma} \exp\left\{-\frac{1}{2\sigma^2}\left(N_{A,B} - \frac{1}{2}\bar{N}\right)^2\right\} \tag{4}$$

with a width σ scaling like $\sigma \propto \sqrt{\bar{N}}$. Within these assumptions, the distribution of the Néel state magnetization Δ is also Gaussian distributed:

$$P(\Delta) = \frac{1}{2\sqrt{\pi}\sigma} \exp\left\{-\frac{1}{4\sigma^2}\Delta^2\right\}. \tag{5}$$

At zero temperature, the magnetization distribution of a given percolation cluster consists of two delta functions located at $M = \pm\Delta$. As shown in figure 1, the effect of a small temperature is a broadening of the two peaks at $\pm\Delta$. The numerical calculations of $P(M)$ shown in figure 1 were carried out using the Swendsen–Wang algorithm [14].

In our toy-model, we first make the approximation that all the geometry dependence of the magnetization response is encoded in the single parameter Δ. This approximation becomes exact in the zero-temperature limit. At a finite but sufficiently low temperature, we still assume this single-parameter description of geometric fluctuations. We further assume that the effect of a finite temperature is a Gaussian broadening of the peaks at $\pm\Delta$ in the magnetization distribution:

$$P_{\Delta,\sigma_\beta}(M) = \frac{1}{2\sqrt{2\pi}\sigma_\beta} \exp\left\{\frac{1}{2\sigma_\beta^2}(M-\Delta)^2\right\} + \frac{1}{2\sqrt{2\pi}\sigma_\beta} \exp\left\{\frac{1}{2\sigma_\beta^2}(M+\Delta)^2\right\}. \tag{6}$$

The thermal broadening σ_β originates from low-temperature excitations above the Néel state. At sufficiently low temperatures, only the lowest energy excitations contribute to σ. If the

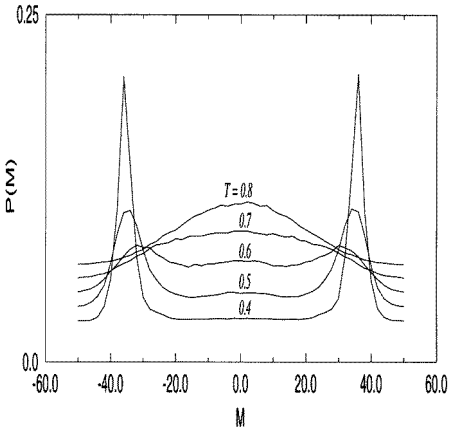

Figure 1. Magnetization distribution of a cluster of $N = 836$ sites,with $\Delta = 36$. This cluster is shown in figure 4 (cluster A).

system was not diluted, these excitations are properly described as a dilute gas of clusters of spins with a wrong orientation with respect to the Néel state. The contribution to σ_β of these excitations is of the order of $\sqrt{N} f(T)$, f being N-independent and behaving like $\ln f(T) \sim -J/T$. It is also well known that long-range low-energy 'droplets' also exist in dilute percolating antiferromagnets, owing to the self-similarity of the structure, and the fact that the order of ramification of the lattice is finite [15]: it costs a finite energy to isolate a cluster of arbitrary size from the rest of the structure. These 'droplet' excitations can be clearly identified in the magnetization distribution of the ferromagnetic Ising model [16]. In fact, we can account for these droplet excitations in an effective distribution of the parameter σ_β over the Néel state magnetization Δ. We shall return to this point in section 2.3.

In (6) we have chosen a Gaussian contribution of thermal excitations. The resulting contribution to the magnetization of these thermal excitations is linear in the magnetic field. In fact, in order to describe how the magnetization saturates for magnetic fields scaling like N^0, one should refine our toy-model to incorporate non-Gaussian tails in the magnetization distribution. Since, as previously mentioned, we are mainly interested in magnetic fields scaling like $T/\sqrt{N}$, these non-Gaussian tails do not play any significant role in this low magnetic field physics.

2.2. Nonlinear effects

Within this toy-model, it is easy to calculate the magnetic field dependence of the average magnetization for a fixed value of Δ. To do so, we note that the magnetization distribution in our toy-model is nothing but the convolution of $P_{\Delta,0}$ and P_{0,σ_β}. As a consequence,

$$\langle \exp(\beta h M)\rangle_{\Delta,\sigma_\beta} = \langle \exp(\beta h M)\rangle_{\Delta,0} \langle \exp(\beta h M)\rangle_{0,\sigma_\beta}$$

from which we deduce the average magnetization for a given value of Δ:

$$M(h) = \sigma_\beta^2 \frac{h}{T} + \Delta \tanh\left(\frac{h\Delta}{T}\right).$$

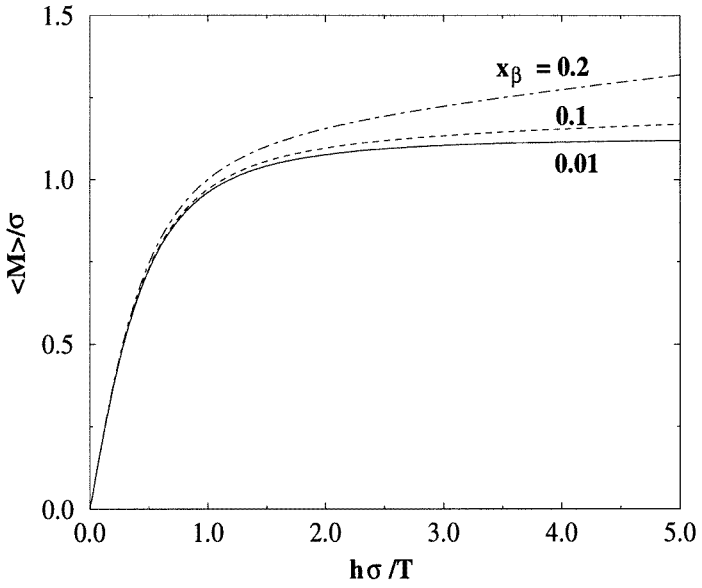

Figure 2. Variations of $\overline{M(h)}/\sigma$ versus $h\sigma/T$ in the toy-model calculation (see (8)), for various values of the parameter $x_\beta = \sqrt{\overline{\sigma_\beta^2}}/\sigma$.

For a fixed Δ, and for a magnetic field smaller than the crossover magnetic field h^* defined as

$$\left(\frac{h^*}{T}\right)^2 = \frac{3(\sigma_\beta^2 + \Delta^2)}{\Delta^4} \tag{7}$$

the magnetization response is linear, whereas it is nonlinear for magnetic fields stronger than h^*. Since Δ and σ_β scale like $\sqrt{N}$, the crossover field h^* is small even for large systems. More precisely, we now average the magnetization over the geometry:

$$\begin{aligned}\overline{M(h)} &= \overline{\sigma_\beta^2}\frac{h}{T} + \int_{-\infty}^{+\infty} P(\Delta)\Delta \tanh\left(\frac{h\Delta}{T}\right) \mathrm{d}\Delta \\ &= \overline{\sigma_\beta^2}\frac{h}{T} + \frac{\sigma}{2\sqrt{\pi}} \int_{-\infty}^{+\infty} u \tanh\left(\frac{h\sigma}{T}u\right) \exp(-u^2/4)\,\mathrm{d}u. \end{aligned} \tag{8}$$

We should distinguish between the two regimes

weak fields: $h \ll T/\sigma \qquad M(h) \simeq (2\sigma^2 + \overline{\sigma_\beta^2})h/T$

intermediate fields: $T/\sigma \ll h \ll T\sigma/\overline{\sigma_\beta^2} \qquad M(h) \simeq 2\sigma/\sqrt{\pi} + \overline{\sigma_\beta^2}h/T.$

As the magnetic field increased from zero, the response to the external field is first linear, and, for magnetic fields of the order of T/σ, crossovers to a nonlinear behaviour. This behaviour is shown in figure 2 for various values of the ratio $x_\beta = \sqrt{\overline{\sigma_\beta^2}}/\sigma$.

2.3. Comparison with simulations

We now compare the predictions of our toy-model for the equilibrium magnetic response of percolation clusters with numerical calculations. We generated 2000 clusters for each value

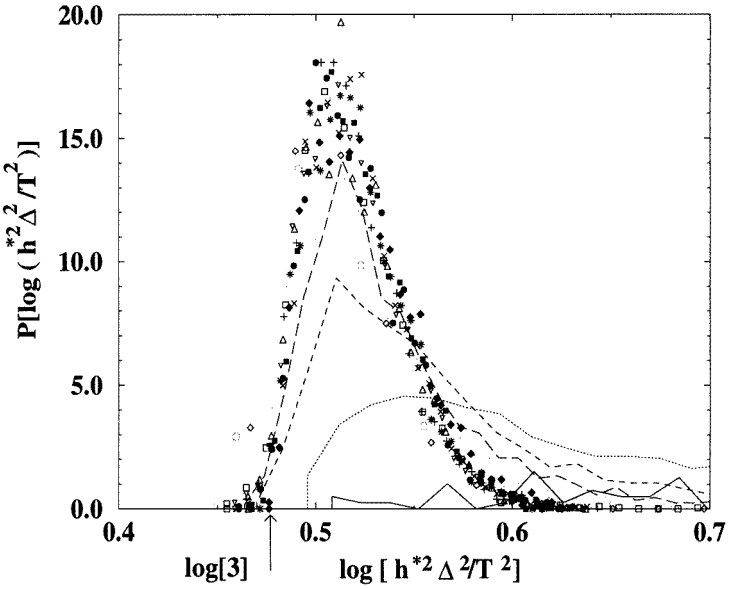

Figure 3. Histogram of $\log((h^*)^2\Delta^2/T^2)$, for different values of the Néel state magnetization Δ. The lines correspond to $\Delta = 1, 2, 3, 4$ and the symbols to values of Δ between 5 and 19. The temperature is $T = 0.4$. 2000 clusters contained in the 20×20 square were generated for each value of Δ.

of the Néel state magnetization Δ. All of these clusters are contained inside the 20×20 square. In order to compare with the toy-model results (7), we have calculated for each of these clusters the crossover field h^* defined by the equality of the linear and cubic terms in the cumulant expansion (3):

$$\left(\frac{h^*}{T}\right)^2 = \left|\frac{6\langle M^2\rangle_0}{\langle M^4\rangle_0 - 3\langle M^2\rangle_0^2}\right| \tag{9}$$

the magnetization distribution in a zero magnetic field being calculated with the Swendsen–Wang algorithm [14]. Figure 3 shows the histogram of $\log((h^*)^2\Delta^2/T^2)$. In the regime $\Delta \gg \sigma_\beta$, equation (7) becomes $(h^*/T)^2 = 3/\Delta^2$: the histograms in figure 3 would be a δ function located on the value $\log 3$. Even if the histograms in figure 3 have a finite width, we note that the scaling $(h^*/T)^2 \sim 1/\Delta^2$ still holds, at least for not too small values of Δ. This suggests that σ_β is not Δ-independent but is rather distributed, and scales on average like Δ. We attribute this behaviour to the existence of low-energy droplet excitations. Since these excitations correspond to large magnetic domains, the magnetization induced by reversing these domains should be coupled to the total Néel state magnetization Δ.

3. Thermoremanent magnetization experiment

In this section, we recall how the function $X(C)$ characterizing the FDT violation can be obtained from the magnetization relaxation in the thermoremanent magnetization experiment. We initially assume linear response. In the presence of a time-dependent magnetic field $h(t)$, the linear contribution to the magnetization is

$$m[h](t) = \int_{-\infty}^{t} R(t, t')h(t')\,\mathrm{d}t' \tag{10}$$

with R the kernel response. We use a working hypothesis

$$R(t,t') = \beta X(C(t,t'))\theta(t-t')\frac{\partial C(t,t')}{\partial t'} \tag{11}$$

a form of the response kernel suggested by the mean-field model studies [6, 8, 9]. The autocorrelation C is

$$C(t_w+\tau,t_w) = \overline{\left\langle \frac{1}{N}\sum_{i,j}\sigma_i(t_w)\sigma_j(t_w+\tau)\right\rangle}. \tag{12}$$

In most of the spin-glass models (for instance: Sherrington–Kirkpatrick model, Edwards–Anderson model), the correlation length is vanishing, the reponse is purely local in space, and the terms $i \neq j$ vanish in (12). In the presence of a finite correlation length, the thermoremanent magnetization is conjugate to the *spatially non-local* autocorrelation (12). From this point of view, (10)–(12) can be safely taken as an extension of $X(C)$ to our problem, in the sense that (i) linear FDT reads $X(C) = 1$ (ii) we recover the usual definition of $X(C)$ in the limit of a zero correlation length.

Barrat [17] recently used an interesting different method to handle spatially non-local responses and nonlinearities: he measured the staggered magnetic response to a random field with a zero mean. In this way, the magnetic response to the random field is linear as a function of the width of the random field distribution, and conjugate to the *local* autocorrelations. We stress that Barrat does not consider the same conjugate quantities as ours, and the functions $X(C)$ are thus different. In particular, we cannot handle symmetry breaking within our framework. However, in the case of the present problem of magnetic systems on percolation clusters, the nonlinearities are quite weak and, as we shall see, we can characterize their effects on dynamics, which could not be possible in the framework of Barrat calculations.

In the thermoremanent magnetization experiment, $h(t)$ is a step function $h(t) = h\theta(t_w - t)$, so that the thermoremanent magnetization reads

$$m(t_w+\tau,t_w) = \beta h \int_0^{C(t_w+\tau,t_w)} X(q)\,\mathrm{d}q$$

where we have assumed $C(t_w+\tau,0) = 0$ (we have indeed checked that this quantity was vanishing in our simulations). The function $X(C)$ is then obtained by differentiating the magnetic response

$$\chi(t_w+\tau,t_w) = \frac{T}{h}m(t_w+\tau,t_w)$$

with respect to the autocorrelation: $X(C) = \mathrm{d}\chi/\mathrm{d}C$. If the waiting time is large enough so that equilibrium has been reached, the magnetic response $\chi(\tau)$ is t_w-independent, $X(C)$ is unity, and we recover the linear FDT:

$$\chi(\tau) = \frac{T}{h}m(\tau) = C_{eq}(\tau). \tag{13}$$

Recently a number of efforts have been devoted to characterize how the FDT is violated in an out-of-equilibrium situation. Analytical solutions were obtained in the framework of mean-field models [6, 8, 9]. The fluctuation–dissipation ratio was also obtained in numerical simulations in various models. For instance, in the case of spin glasses, Franz and Rieger [18] have analysed the Edwards–Anderson model in three dimensions; more recently, Marinari *et al* [19] have studied the FDT violation in three- and four-dimensional Gaussian Ising spin glasses, and shown that the fluctuation–dissipation ration $X(C)$ is, in

these models, equal to the static Parisi function $x(C)$. A model of fragile glass was also studied recently [20].

As explained in section 2, the magnetic response of percolating dilute antiferromagnets is not linear for magnetic fields of the order of $T/\sqrt{N}$. In the absence of linear response, the equilibrium magnetization can be expanded in powers of the magnetic field h, the coefficients of this expansion being the cumulants of the magnetization distribution (see equation (3)). Following the work of Gallavotti and Cohen [21] in the context of chaotic systems in classical mechanics, Kurchan [23] recently proposed an extension of the FDT to incorporate the effects of nonlinear response. However, we cannot use this generalization here in our Monte Carlo simulations since this would involve the calculation of the time-dependent magnetization distribution, included the tail where the magnetization is opposite to the magnetic field [22]. The study of this nonlinear FDT and its violations in the context of glassy dynamics goes beyond the scope of computer resources available at present. This is why we adopt here a more phenomenological approach, consisting in generalizing (11) to the nonlinear regime:

$$R_h(t,t') = \beta X_h(C(t,t'))\theta(t-t')\frac{\partial C(t,t')}{\partial t'}$$

with a magnetic-field-dependent X_h.

In the presence of nonlinearities and out-of-equilibrium dynamics, $X_h(C)$ contains contributions both from the nonlinearities and the ageing dynamics. However, in the limit of large waiting times, the system has equilibrated and thus only the nonlinearities contribute to $X_h(C)$. In the opposite limit of small waiting times, the nonlinearities do not contribute to $X(C)$, and, in this limit, a contact can be made with FDT violations in other systems, especially Euclidean coarsening dynamics [17].

4. Numerical results for $X(C)$

We now present our numerical calculations of $X(C)$. Our simulations were carried out on two clusters: a cluster A with $N = 836$ sites, $\Delta = 36$, and a smaller cluster B with $N = 294$ sites and $\Delta = 16$. These two clusters are shown in figure 4.

We first present in section 4.1 the equilibrium dynamics: the waiting time is long enough for the system to have equilibrated in the external magnetic field, and, on the basis of the arguments presented in section 2, we expect sensible nonlinear effects. In fact, the relaxation time is finite even in the thermodynamic limit (interrupted ageing). As the size of the system increases, the relaxation time will first increase, owing to zero energy barriers scaling like $J \ln N$ [10], and saturate when the linear size $N^{1/d}$ becomes larger than the correlation length given by [13]

$$\xi_T \sim \exp\left(\frac{2J\nu_P}{T}\right)$$

with ν_P the percolation critical exponent. The limit of small waiting times is presented in section 4.2. In this situation, the magnetic response is linear. The combined effects of nonlinearities and out-of-equilibrium responses arising for intermediate waiting times are presented in section 4.3. Finally, the dependence on τ of the autocorrelation and the magnetic response are presented in section 4.4.

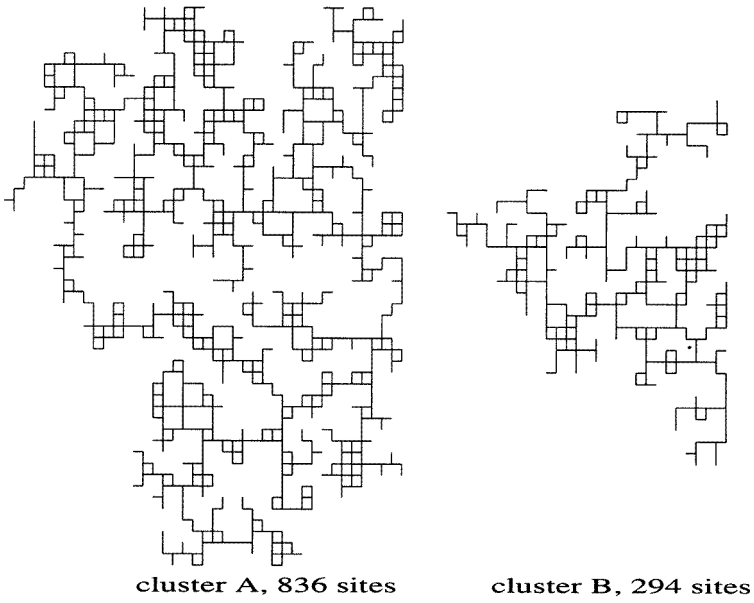

Figure 4. The two clusters that we studied. The cluster A contains $N = 836$ sites, and $\Delta = 36$. The cluster B contains $N = 294$ sites, and $\Delta = 16$.

4.1. Large waiting times: equilibrium dynamics and nonlinear response

We first examine the regime of a large waiting time t_w, large enough for the magnetic response to be independent on t_w. In practice, we systematically checked that the magnetic response was unchanged when the waiting time was increased by a factor of 10. The magnetic response χ_h is plotted as a function of the autocorrelation C in figure 5 for the clusters A and B. We clearly observe on figure 5 important nonlinear effects since the magnetic response χ_h depends explicitly on the magnetic field h, even at the relatively high temperature $T = 0.8$. In the short-time limit, we observe a behaviour of the type $\chi_h(C) = C - C_h^{(0)}$, whereas in the long time limit, $\chi_h(C) = X_h^{(0)} C$. In order to interpolate between these two behaviours, we have fitted our numerical results to the form

$$X_h(C) = \frac{\mathrm{d}\chi_h(C)}{\mathrm{d}C} = (1 - X_h^{(0)}) f_{C_h^*,\lambda_h}(C) + X_h^{(0)} \tag{14}$$

with

$$f_{C_h^*,\lambda_h}(C) = \left(1 + \exp\left(-\frac{C - C_h^*}{\lambda_h}\right)\right)^{-1}$$

where λ_h controls the width of the crossover between the short- and long-time regimes, and $C_h^* = C_h^{(0)}/(1 - X_h^{(0)})$. The fits obtained in this way are shown in figure 5, and, once the three parameters have been adjusted, a very good agreement with the simulation data is obtained. The variations of $X_h(C)$ deduced from the fits are shown in figure 6 for the same simulations as in figure 5. We observe in figure 6 that $X_h(C)$ crossovers from unity at short times to a finite value $X_h^{(0)}$ in the long-time relaxation. If the response to the external magnetic field was linear, one would expect that $X(C) = 1$. Even though we could not address this question here, we expect a nonlinear FDT of the type [23] to hold in the long waiting time limit.

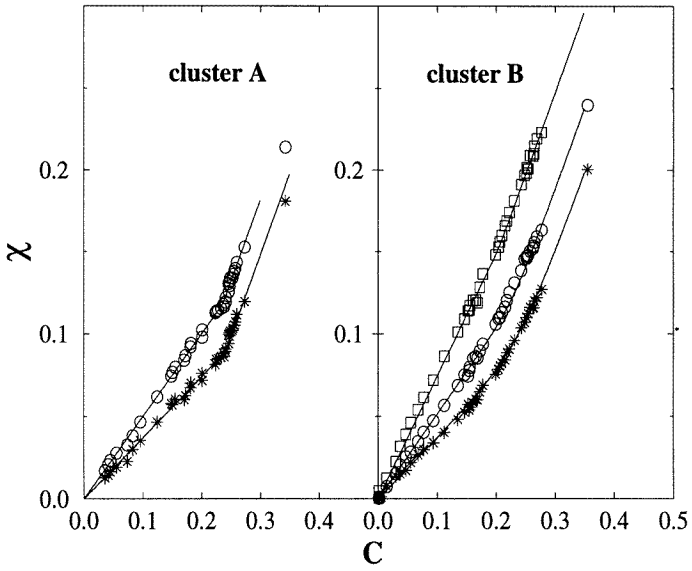

Figure 5. Variation of the magnetic response $\chi_h(C)$ versus the autocorrelation C in equilibrium relaxation. The temperature is $T = 0.8$, and the waiting time is $t_w = 10^5$. The magnetic fields are $h = 0.1$ (squares), $h = 0.2$ (circles) and $h = 0.3$ (crosses). The curves have been fitted using the procedure described in the text.

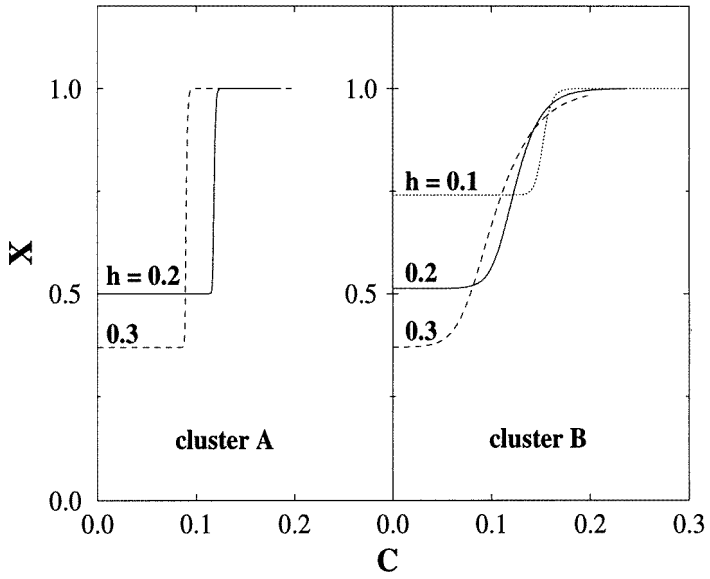

Figure 6. Variation of $X_h(C)$ versus C in equilibrium relaxation. The temperature is $T = 0.8$. The variations of $X_h(C)$ are deduced from the simulations presented in figure 5.

4.2. Small waiting times: out-of-equilibrium dynamics and linear response

In the short waiting time limit, the thermoremanent magnetization is linear as a function of the magnetic field. We have shown in figure 7 the variations of the magnetic response

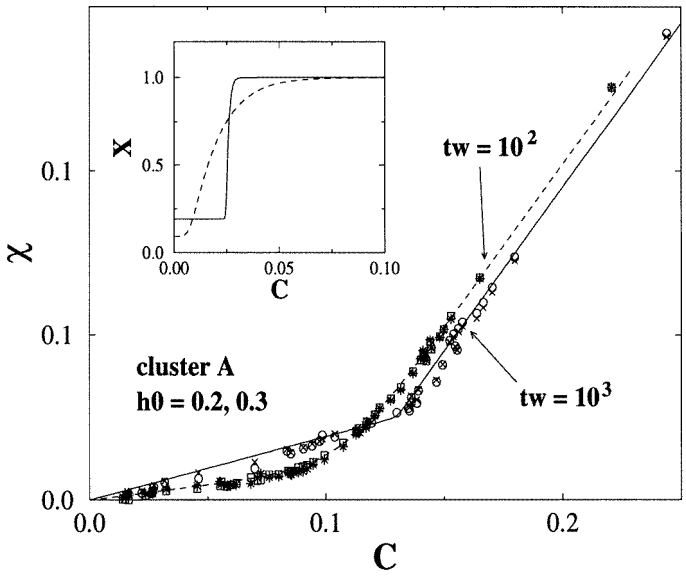

Figure 7. Variations of the magnetic response $\chi(C)$ versus the autocorrelation C in the short waiting time limit ($t_w = 10^2, 10^3$), and $h = 0.2, 0.3$. The corresponding variations of $X(C)$ are shown in the inset.

χ versus the autocorrelation C for the two values of the magnetic field $h = 0.2, 0.3$, and $t_w = 10^2, 10^3$. Linear response is clearly observed. The variations of $X(C)$ are shown in the inset of figure 7. Interestingly, the variations of $X(C)$ in this situation where out-of-equilibrium effects are dominant are qualitatively the same as those in section 4.1: X crossovers from unity at short times to a finite value in the long-time limit. We have no understanding of the reason why the variations of $X(C)$ are qualitatively the same in the small and large waiting time limits, where deviations from linear FDT originate respectively from the out-of-equilibrium dynamics and nonlinear response.

The fact that $X(C)$ is finite in the ageing regime is a quite noticeable difference with Euclidean coarsening [17], where X is vanishing in the ageing regime (the linear response kernel R in (10) is zero in this regime). The long-term memory of coarsening dynamics on percolating structures is thus stronger than for Euclidean dynamics, which is maybe not surprising on the general grounds recalled in the introduction: a 'droplet' of size N has a zero-temperature energy barrier scaling such as $\ln N$ [10–12], and a finite energy of the order of $2\mathcal{C}J$, $\mathcal{C}$ being the order of ramification [15].

4.3. Intermediate waiting times: out-of-equilibrium dynamics and nonlinear response

In order to examine the conjugate effects of nonlinearities in the magnetization response and out-of-equilibrium dynamics, we carried out the thermoremanent magnetization simulation with the cluster B at the temperature $T = 0.55$, and for a waiting time $t_w = 10^6$. The results are shown in figure 8, with τ up to 10^7. We have checked that equilibrium was not reached by carrying a simulation with a waiting time $t_w = 10^7$. On the other hand, the magnetic response χ_h depends explicitly on the magnetic field h, as is visible in figure 8. We observe that $X_h(C)$ can still be fitted by the form (14), even though we could not reach very small values of the correlation and magnetic responses, even for $\tau = 10^7$.

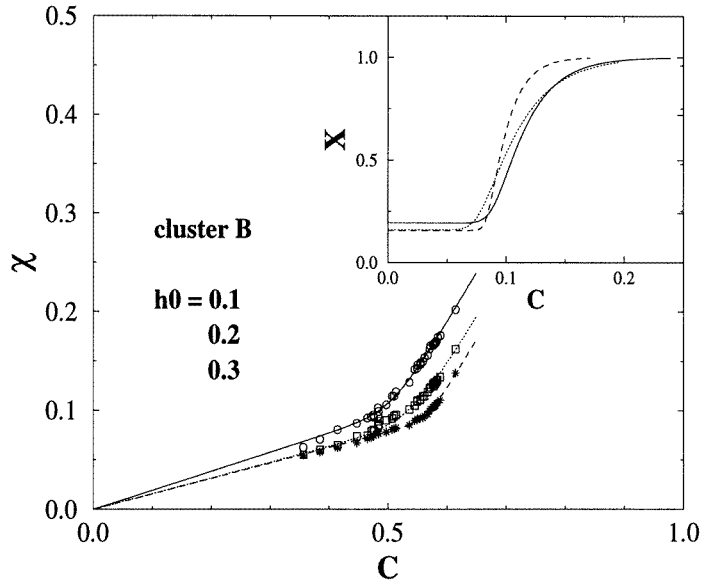

Figure 8. Variations of the magnetic response $\chi_h(C)$ versus the autocorrelation C for the cluster B, $T = 0.55$, $t_w = 10^6$, $h = 0.1$ (circles), $h = 0.2$ (squares), 0.3 (crosses). The inset shows the corresponding variations of $X(C)$.

4.4. τ-dependence of $\chi(t_w + \tau, t_w)$ and $C(t_w + \tau, t_w)$

In spin-glass models, the short-time regime $\chi(t_w + \tau, t_w) = C(t_w + \tau, t_w) - C^{(0)}(t_w)$ is valid up to a time τ^* of the order of the waiting time t_w [18]. As shown in figure 9, we indeed observe such a dependence of τ^* in the out-of equilibrium situation: τ^* is of the order of 10^2 for $t_w = 10^2$, and of the order of 10^3 for $t_w = 10^3$. However, for larger waiting times, nonlinearities significantly reduce τ^* ($\tau^* \simeq 10^3$ for $t_w = 10^5$ in figure 9). We observe in figure 10 in the case $t_w = 10^5$, $T = 0.8$ (equilibrium situation) that τ^* is also a function of the magnetic field h (the value of τ^* for $h = 0.1$ is one order of magnitude larger than for $h = 0.2$). This effect is also visible in the out-of-equilibrium simulation shown in figure 10 ($T = 0.55$). However, from our simulations, we cannot make a precise statement on the variations of τ^* as a function of h for large waiting times.

5. Conclusions

We have thus carried out Monte Carlo simulations of the violation of the linear FDT in dilute percolating antiferromagnets. We have shown that these systems exhibit nonlinear response for magnetic fields of the order of $T/\sqrt{N}$. In the small waiting time regime, the thermoremanent magnetization is linear in the magnetic field, but depends explicitly on the waiting time. On the other hand, for sufficiently large waiting times, the system has equilibrated (interrupted ageing), and the magnetic response is nonlinear.

In the strongly out-of-equilibrium regime, the function $X(C)$ is non-vanishing in the ageing regime, in contrast to the usual Euclidean coarsening behaviour. This shows that coarsening on percolation clusters has a stronger long-term memory than Euclidean coarsening [17], where X vanishes in the ageing regime. This stronger memory kernel originates from the existence of low-energy large-scale 'droplet' excitations with zero-

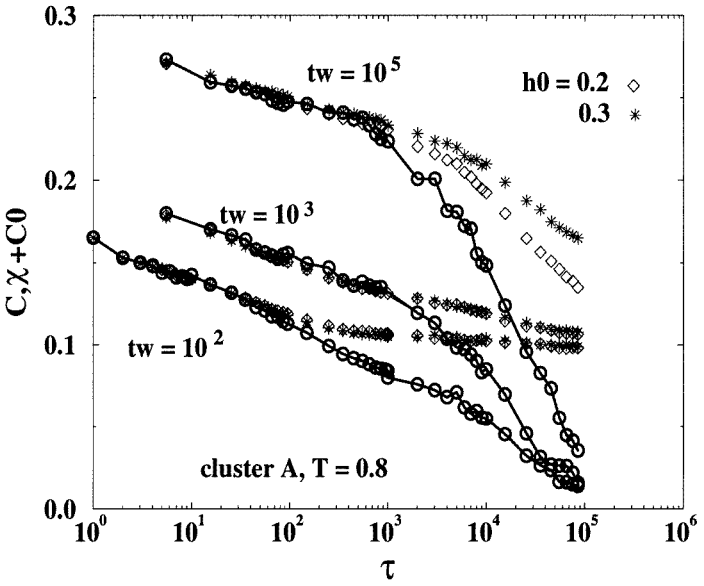

Figure 9. Variations of $\chi(t_w + \tau, t_w) + C^{(0)}(t_w)$ (diamonds: $h = 0.2$, crosses: $h = 0.3$) and $C(t_w + \tau, t_w)$ (full curves) versus τ. The waiting times are $t_w = 10^2, 10^3, 10^5$. The temperature is $T = 0.8$.

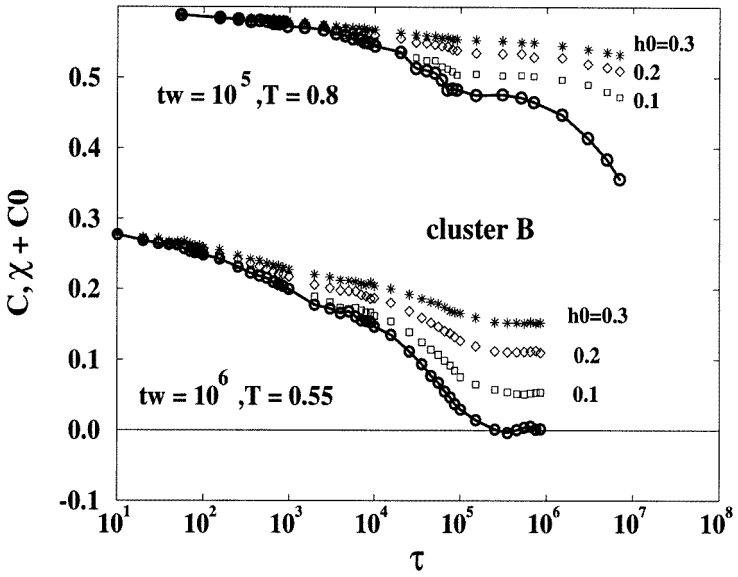

Figure 10. Variations of $\chi(t_w + \tau, t_w) + C^{(0)}(t_w)$ (squares: $h = 0.1$, diamonds: $h = 0.2$, crosses: $h = 0.3$) and $C(t_w + \tau, t_w)$ (full curves) versus τ. The waiting times are $t_w = 10^5$ ($T = 0.8$), and $t_w = 10^6$ ($T = 0.55$).

temperature energy barriers scaling such as $J \ln N$. Interestingly, within the droplet picture for finite-dimensional spin-glass systems [4, 5], spin-glass dynamics can be thought of

as a domain of growth dynamics in the presence of disorder and frustration†. We refer the reader to [24] for a detailed comparison between the droplet picture and numerical simulations of finite-dimensional spin-glass models. In contrast to these finite-dimensional spin-glass models, we studied an *unfrustrated* model in a fluctuating geometry, with a finite but possibly long relaxation time. Despite interrupted ageing, the kernel response shows a relatively similar behaviour to finite-dimensional spin-glass models in three [18] and four [19] dimensions, and structural glasses [20].

Moreover, we have also studied the long waiting time relaxation, where the system is close to equilibrium. The effects of nonlinearities have been studied by assuming that the relation between the thermoremanent magnetization and the autocorrelation had the same form as in the linear regime, except for a magnetic-field-dependent $X_h(C)$. The variations of $X_h(C)$ are qualitatively similar whatever the strength of the nonlinearities.

Acknowledgments

RM thanks A Barrat, L F Cugliandolo, S Franz, P C W Holdsworth and J Kurchan for stimulating discussions. Part of the calculations presented here were carried out on the CRAY T3E computer of the Centre de Calcul Vectoriel Grenoblois of the Commissariat à l'Energie Atomique.

References

[1] Lundgren L, Svedlindh P, Norblad P and Beckman O 1983 *Phys. Rev. Lett.* **51** 911
Norblad P, Lundgren L, Svedlindh P and Sandlund L 1988 *Phys. Rev.* B **33** 645
Lundgren L 1988 *J. Physique Coll.* **49** C8-1001 and references therein
[2] Alba M, Ocio M and Hamman J 1986 *Europhys. Lett.* **2** 45
Alba M, Ocio M and Hamman J 1985 *J. Physique Lett.* **46** L1101
Alba M, Hamman J, Ocio M and Refregier P 1987 *J. Appl. Phys.* **61** 3683
Vincent E, Hamman J and Ocio M 1992 *Recent Progress in Random Magnets* ed D H Ryan (Singapore: World Scientific)
[3] Bouchaud J P, Cugliandolo L F, Mézard M and Kurchan J 1997 Out-of-equilibrium dynamics in spin-glasses and other glassy systems *Spin Glasses and Random Field* ed A P Young (Singapore: World Scientific)
[4] Fisher D S and Huse D A 1986 *Phys. Rev. Lett.* **56** 1601
Fisher D S and Huse D A 1988 *Phys. Rev.* B **38** 373
[5] Koper G J and Hilhorst H J 1989 *Physica* **155A** 431
[6] Cugliandolo L F and Kurchan J 1993 *Phys. Rev. Lett.* **71** 173
Cugliandolo L F and Kurchan J 1994 *J. Phys. A: Math. Gen.* **27** 5749
[7] Bouchaud J P 1992 *J. Physique* I 1992 **2** 1705
Bouchaud J P, Vincent E and Hamman J 1994 *J. Physique* I **4** 139
Bouchaud J P and Dean D S 1995 *J. Physique* I **5** 265
[8] Baldassari A, Cugliandolo L F, Kurchan J and Parisi G 1995 *J. Phys. A: Math. Gen.* **28** 1831
[9] Cugliandolo L F and Dean D S 1995 *J. Phys. A: Math. Gen.* **28** 4213
[10] Rammal R and Benoît A 1985 *J. Physique Lett.* **46** L667
Rammal R and Benoît A 1985 *Phys. Rev. Lett.* **55** 649
[11] Rammal R 1985 *J. Physique* **46** 1837
[12] Henley C L 1985 *Phys. Rev. Lett.* **54** 2030
[13] Coniglio A 1981 *Phys. Rev. Lett.* **46** 250
[14] Swendsen R H and Wang J S 1986 *Phys. Rev. Lett.* **57** 2606
Swendsen R H and Wang J S 1987 *Phys. Rev. Lett.* **58** 86

† We stress that the spin-glass droplet model [4] has quite different elements from the droplets in the present percolation cluster model. For instance, the energy barriers in [4] are power law of the droplet volume whereas they have a logarithmic dependence in percolation clusters.

See also Swendsen R H, Wang J S and Ferrenberg A M 1992 *The Monte Carlo Method in Condensed Matter Physics (Topics in Applied Physics 71)* ed K Binder (Berlin: Springer)
[15] Kirkpatrick S 1979 *Proc. Les Houches Summer School on Ill Condensed Matter Physics* ed R Ballian, R Maynard and G Toulouse (Amsterdam: North-Holland)
[16] Mélin R 1996 *J. Physique* I **6** 793
[17] Barrat A 1997 *Report* cond-mat/9710069
[18] Franz S and Rieger H 1995 *J. Stat. Phys.* **79** 749
[19] Marinari E, Parisi G, Ricci-Tersenghi F and Ruiz-Lorenzo J J 1997 *Report* cond-mat/9710120
[20] Parisi G 1997 *Phys. Rev. Lett.* **79** 3660
[21] Gallavotti G and Cohen E G D 1995 *Phys. Rev. Lett.* **74** 2694
Gallavotti G and Cohen E G D 1995 *J. Stat. Phys.* **80** 931
Gallavotti G 1996 *Phys. Rev. Lett.* **77** 4334
[22] The Gallavotti-Cohen FDT was indeed tested numerically in the context of classical chaotic dynamics, see for instance Bonetto F, Gallavotti G and Garrido P L 1996 Chaotic principle: an experimental test #96-154 in http://www.ma.utexas.edu.
[23] Kurchan J 1997 *Report* cond-mat/9709304
[24] Rieger H 1993 *J. Phys. A: Math. Gen.* **26** L615
Kisher J, Santen L, Schreckenberg M and Rieger H 1996 *Phys. Rev.* B **53** 6418